Inorg. Chem. **2004**, *43*, 92–100

Module-Based Assembly of Copper(II) Chloranilate Compounds: Syntheses, Crystal Structures, and Magnetic Properties of $\{[Cu_2(CA)(terpy)_2][Cu(CA)_2]\}_n$ and $\{[Cu_2(CA)(terpy)_2(dmso)_2][Cu(CA)_2(dmso)_2](EtOH)\}_n$ (H_2CA = Chloranilic Acid, terpy = 2,2′:6′,2″-Terpyridine, dmso = Dimethyl Sulfoxide)

Mitsuhiro Kawahara,[†] Md. Khayrul Kabir,[‡,§] Koichi Yamada,[‡] Keiichi Adachi,[‡] Hitoshi Kumagai,[†,||] Yasuo Narumi,[⊥] Koichi Kindo,[⊥] Susumu Kitagawa,[#] and Satoshi Kawata*[,‡]

Department of Chemistry, Graduate School of Scienec, Tokyo Metropolitan University, Minami Ohsawa, Hachiouji, Tokyo 192-0397, Japan, Department of Chemistry, Graduate School of Science, Osaka University, Machikaneyamacho Toyonaka, Osaka, 560-0043, Japan, Research Center for Materials Science at Extreme Conditions, Osaka University, Machikaneyamacho Toyonaka, Osaka, 560-8531, Japan, and Department of Synthetic Chemistry and Biological Chemistry, Graduate School of Engineering, Kyoto University, Yoshida, Saikyo-ku, Kyoto 606-8501, Japan

Received September 4, 2003

Two new copper(II) compounds of chloranilate and 2,2′:6′,2″-terpyridine have been synthesized, and the structures have been solved by the single-crystal X-ray diffraction method. The crystal structure of $\{[Cu_2(CA)(terpy)_2][Cu(CA)_2]\}_n$ (**1**), where H_2CA = chloranilic acid and terpy = 2,2′:6′,2″-terpyridine, consists of two modules, the dimer unit $[Cu_2(CA)(terpy)_2]^{2+}$ and the anionic mononuclear unit $[Cu(CA)_2]^{2-}$, forming an alternated chain. The chain is stabilized by semicoordinating and additional but efficient secondary bonding interactions. The crystal structure of $\{[Cu_2(CA)(terpy)_2(dmso)_2][Cu(CA)_2(dmso)_2](EtOH)\}_n$ (**2**), where dmso = dimethyl sulfoxide, consists of solvent molecules and two discrete modules, the dimer unit $[Cu_2(CA)(terpy)_2(dmso)_2]^{2+}$ and the anionic mononuclear unit $[Cu(CA)_2(dmso)_2]^{2-}$. The dimer units form a layer by secondary bonding interactions, and the monomer units and ethanol molecules are introduced between the layers. The magnetic properties of **1** and **2** have been investigated in the temperature range 2.0–300 K. A weak ferromagnetic interaction was observed in **1**, $J_a = 2.36\ cm^{-1}$ and $zJ_b = -0.68\ cm^{-1}$ while no exchange coupling was observed in **2**.

Introduction

Crystal engineering with desired functions and fascinating topological architectures has become an area of increasing interest in recent years.[1−8] One of the most significant approaches in the field is to use robust modules or motifs to design supramolecular architectures.[9−12] In this context, discrete modules for inorganic−organic hybrid materials are linked to larger networks through coordinate bonds, covalent

* To whom correspondence should be addressed. Fax: +81-6-6850-5409. E-mail: kawata@chem.sci.osaka-u.ac.jp.
[†] Tokyo Metropolitan University.
[‡] Osaka University.
[§] Present address: Department of Chemistry, University of Victoria, British Columbia V8W 3V6, Canada.
[⊥] Osaka University (Research Center for Materials Science at Extreme Conditions).
[#] Kyoto University.
[||] Present address: Institute for Molecular Science (IMS), Nishigounaka 38, Myoudaiji, Okazaki 444-8585, Japan.

(1) Lehn, J.-M. *Supramolecular Chemistry*; VCH: Weinheim, Germany, 1995.
(2) Desiraju, G. R. *Nature* **2001**, *412*, 397.
(3) Desiraju, G. R. *Acc. Chem. Res.* **2002**, *35*, 565.
(4) Aakeöy, C. B.; Seddon, K. R. *Chem. Soc. Rev.* **1993**, *22*, 397.
(5) Braga, D.; Desiraju, G. R.; Miller, J. S.; Orpen, A. G.; Price, S. L. *CrystEngComm* **2002**, *4*, 500.
(6) Braga, D.; Maini, L.; Polito, M.; Scaccianoce, L.; Cojazzi, G.; Grepioni, F. Coord. *Chem. Rev.* **2001**, *216*, 225.
(7) Moulton, B.; Zaworotko, M. J. *Chem. Rev.* **2001**, *101*, 1629.
(8) Sharma, C. V. K. *Cryst. Growth Des.* **2002**, *2*, 465.
(9) Desiraju, G. R. *Angew. Chem., Int. Ed. Engl.* **1995**, *34*, 2311.
(10) Yagi, O. M.; Li, G.; Li, H. *Nature* **1995**, *378*, 703.
(11) Eddaoudi, M.; Kim, J.; Rosi, N.; Vodak, D.; Wachter, J.; O'Keeffe, M.; Yaghi, O. M. *Science* **2002**, *295*, 469.
(12) Eddaoudi, M.; Moler, D. B.; Li, H.; Chen, B.; T. M. Reineke, M. O. k.; Yaghi, O. M. *Acc. Chem. Res.* **2001**, *34*, 319.

10.1021/ic035044y CCC: $27.50
Published on Web 12/05/2003

bonds, or other intermolecular secondary bonding interactions, such as hydrogen bonding, $\pi-\pi$ stacking interactions, etc.[13−19] Supramolecular chemistry has advanced to a stage at which we can design and construct molecular solids with specific network topologies. Especially hybrid polynuclear transition metal complexes have offered promising perspectives toward developing new functional materials.[20−26] A promising strategy of the construction of polynuclear systems is the hybrid inorganic/organic self-assembly approach in which the inorganic elements are linked by organic bridges, and many excellent examples have been reported.[27−34]

It is well-known that the dianion of 2,5-dichloro-3,6-dihydroxy-1,4-benzoquinone (chloranilic acid, H_2CA) can coordinate to metal ions in both the bidentate and the bis-bidentate fashions.[35−41] As a result, CA^{2-} can be used as both the terminal and the bridging ligands. The former affords monomeric crystal structures whereas the later allows extending arrays such as a dimer, one-dimensional (1D) chain, or two-dimensional (2D) layer structure by using coordination bonding interactions (Scheme 1, type A).[42−53]

Scheme 1

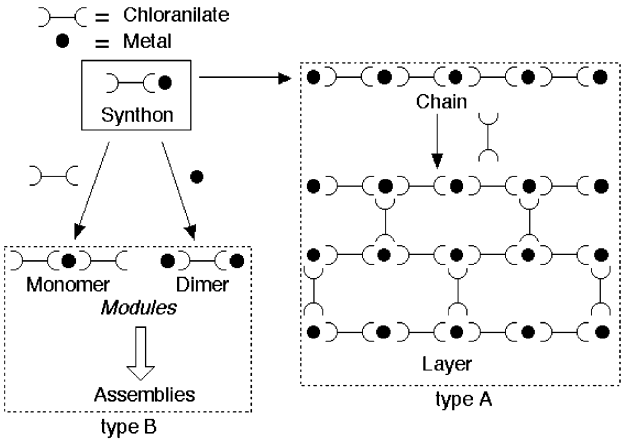

However, the monomer compounds can also be built up to higher dimensional structures by secondary bonding interactions, such as hydrogen-bonding interactions, $\pi-\pi$ stacking interactions, etc.[13,54−57] These polynuclear compounds are uniformly built from a common synthon (metal−chloranilate: M−CA).

The simple synthon makes various kinds of architectures through self-assembling processes, and the versatility of the chloranilic acid prompts us to construct new assembled compounds which consist of different kinds of modules (monomer, dimmer, etc.) that are made up of the common synthon (Scheme 1, type B). Moreover, the extension of this chemistry would afford intriguing crystal structures and physicochemical properties if the two forms in the same crystal structures will offer different properties.

In this study we have synthesized two compounds of copper(II) with chloranilate and 2,2′:6′,2″-terpyridine using

(13) Nagayoshi, K.; Kabir, M. K.; Tobita, H.; Honda, K.; Kawahara, M.; Katada, M.; Adachi, K.; Nishikawa, H.; Ikemoto, I.; Kumagai, H.; Hosokoshi, Y.; Inoue, K.; Kitagawa, S.; Kawata, S. *J. Am. Chem. Soc.* **2003**, *125*, 221.
(14) Kitaura, R.; Seki, K.; Akiyama, G.; Kitagawa, S. *Angew. Chem., Int. Ed.* **2003**, *42*, 428.
(15) Kitaura, R.; Kitagawa, S.; Kubota, Y.; Kobayashi, T. C.; Kindo, K.; Mita, Y.; Matsuo, A.; Kobayashi, M.; Chang, H.-C.; Ozawa, T. C.; Suzuki, M.; Sakata, M.; Takata, M. *Science* **2002**, *298*, 2358.
(16) Moulton, B.; Lu, J.; Hajndl, R.; Hariharan, S.; Zaworotko, M. J. *Angew. Chem., Int. Ed.* **2002**, *41*, 2821.
(17) Hollingsworth, M. D. *Science* **2002**, *295*, 2410.
(18) Moorthy, J. N.; Natarajan, R.; Mal, P.; Venugopalan, P. J. *Am. Chem. Soc.* **2002**, *124*, 6530.
(19) Robson, R. *J. Chem. Soc., Dalton Trans.* **2000**, 3735.
(20) Kishida, H.; Matsuzaki, H.; Okamoto, H.; Manabe, T.; Yamashita, M.; Taguchi, Y.; Tokura, Y. *Nature* **2000**, *405*, 929.
(21) Clérac, R.; Miyasaka, H.; Yamashita, M.; Coulon, C. *J. Am. Chem. Soc.* **2002**, 12837.
(22) Coronado, E.; Galán-Mascarós, J. R.; Gómez-García, C. J.; Laukhin, V. *Nature* **2000**, *408*, 447.
(23) Holman, K. T.; Pivovar, A. M.; Ward, M. D. *Science* **2001**, *294*, 1907.
(24) MacDonald, J. C.; Dorrestein, P. C.; Pilley, M. M.; Foote, M. M.; Lundburg, J. L.; Henning, R. W.; Schultz, A. J.; Manson, J. L. *J. Am. Chem. Soc.* **2000**, *122*, 11692.
(25) Adachi, K.; Kawata, S.; Kabir, M. K.; Kumagai, H.; Inoue, K.; Kitagawa, S. *Chem. Lett.* **2001**, 50.
(26) Kawata, S.; Adachi, K.; Sugiyama, Y.; Kabir, M. K.; Kaizaki, S. *CrystEngComm* **2002**, *4*, 496.
(27) Seidel, S. R.; Stang, P. J. *Acc. Chem. Res.* **2002**, *35*, 972.
(28) Kuehl, C. J.; Kryschenko, Y. K.; Radhakrishnan, U.; Seidel, S. R.; Huang, S. D.; Stang, P. J. *Proc. Nat. Acad. Sci. U.S.A.* **2002**, *99*, 4932.
(29) Mbindyo, J. K. N.; Mallouk, T. E.; Mattzela, J. B.; Kratochvilova, I.; Razavi, B.; Jackson, T. N.; Mayer, T. S. *J. Am. Chem. Soc.* **2002**, *124*, 4020.
(30) Kim, K. *Chem. Soc. Rev.* **2002**, 31, 96.
(31) Halder, G. J.; Kepert, C. J.; Moubaraki, B.; Murray, K. S.; Cashion, J. D. *Science* **2002**, *298*, 1762.
(32) Berlinguette, C. P.; Vaughn, D.; Cañada-Vilalta, C.; Galán-Mascarós,J. R.; Dunbar, K. R. *Angew. Chem., Int. Ed.* **2003**, *42*, 2289.
(33) Evans, O. R.; Lin, W. *Acc. Chem. Res*. **2002**, *35*, 511.
(34) Abourahma, H.; Moulton, B.; Kravtsov, V.; Zaworotko, M. J. *J. Am. Chem. Soc.* **2002**, *124*, 9990.
(35) Kawata, S.; Kitagawa, S. *Coord. Chem. Rev.* **2002**, *224*, 11.
(36) Kobayashi, H.; Haseda, T.; Kanda, E.; Kanda, S. *J. Phys. Soc. Jpn.* **1963**, *18*, 349.
(37) Wrobleski, J. T.; Brown, D. B. *Inorg. Chem.* **1979**, *18*, 498.
(38) Verdaguer, M.; Michalowicz, A.; Girerd, J. J.; Alberding, N.; Kahn, O. *Inorg. Chem.* **1980**, *19*, 3271.
(39) Robl, C.; Kuhs, W. F. *J. Solid State Chem.* **1989**, *79*, 46.
(40) Robl, C.; Weiss, A. *Mater. Res. Bull.* **1987**, *22*, 497.
(41) Weiss, A.; Riegler, E.; Robl, C. *Z. Naturforsch.* **1986**, *41b*, 1501.
(42) Pierpont, C. G.; Francesconi, L. C.; Hendrickson, D. N. *Inorg. Chem.* **1977**, *16*, 2367.
(43) Pierpont, C. G.; Francesconti, L. C.; Hendrickson, D. *Inorg. Chem.* **1978**, *17*, 3470.
(44) Tinti, F.; Verdaguer, M.; Kahn, O.; Savariault, J.-M. *Inorg. Chem.* **1987**, *26*, 2380.
(45) Folgado, J. V.; Ibáñez, R.; Coronado, E.; Beltrán, D.; Saavariault, J. M.; Galy, J. *Inorg. Chem.* **1988**, *27*, 19.
(46) Kawata, S.; Kitagawa, S.; Kondo, M.; Furuchi, I.; Munakata, M. *Angew. Chem., Int. Ed. Engl.* **1994**, *33*, 1759.
(47) Kawata, S.; Kitagawa, S.; Kumagai, H.; Ishiyama, T.; Honda, K.; Tobita, H.; Adachi, K.; Katada, M. *Chem. Mater.* **1998**, *10*, 3902.
(48) Kawata, S.; Kitagawa, S.; Kumagai, H.; Kudo, C.; Kamesaki, H.; Ishiyama, T.; Suzuki, R.; Kondo, M.; Katada, M. *Inorg. Chem.* **1996**, *35*, 4449.
(49) Kumagai, H.; Kawata, S.; Kitagawa, S. *Inorg. Chim. Acta* **2002**, *337*, 387.
(50) Kabir, M. K.; Kawahara, M.; Kumagai, H.; Adachi, K.; Kawata, S.; Ishii, T.; Kitagawa, S. *Poyhedron* **2001**, *20*, 1417.
(51) Kabir, M. K.; Kawahara, M.; Adachi, K.; Kawata, S.; Ishii, T.; Kitagawa, S. *Mol. Cryst. Liq. Cryst.* **2002**, *376*, 65.
(52) Abrahams, B. F.; Lu, K. D.; Moubaraki, B.; Murray, K. S.; Robson, R. *J. Chem. Soc., Dalton Trans.* **2000**, 1793.
(53) Abrahams, B. F.; Coleiro, J.; Ha, K.; Hoskins, B. F.; Orchard, S. D.; Robson, R. *J. Chem. Soc., Dalton Trans.* **2002**, 1586.
(54) Kawata, S.; Kumagai, H.; Adachi, K.; Kitagawa, S. *J. Chem. Soc., Dalton Trans.* **2000**, 2409.
(55) Kawata, S.; Kumagai, H.; Kitagawa, S.; Honda, K.; Enomoto, M.; Katada, M. *Mol. Cryst. Liq. Cryst.* **1996**, *286*, 51.
(56) Kabir, M. K.; Kawata, S.; Adachi, K.; Tobita, H.; Miyazaki, N.; Kumagai, H.; Katada, M.; Kitagawa, S. *Mol. Cryst. Liq. Cryst.* **2000**, *341*, 491.
(57) Kabir, M. K.; Miyazaki, N.; Kawata, S.; Adachi, K.; Kumagai, H.; Inoue, K.; Kitagawa, S.; Iijima, K. *Coord. Chem. Rev.* **2000**, *198*, 157.

the self-assembling technique. The crystallographic and magnetic characterization of these compounds are also described. The crystal structures of these compounds consist of different kinds of modules which are made of the simple synthon. Among the distinct factors involved in the syntheses of these compounds, the solvent has been reported to highly influence the resulting frameworks.

Experimental Section

Materials. Copper(II) sulfate pentahydrate, $CuSO_4 \cdot 5H_2O$, chloranilic acid, and 2,2′:6′,2″-terpyridine were purchased from commercial sources and used as received.

Syntheses. $\{[Cu_2(CA)(terpy)_2][Cu(CA)_2]\}_n$ **(1).** An aqueous solution (2 mL) of copper(II) sulfate pentahydrate (1 mmol·L^{-1}) was transferred to a glass tube, and then an water−ethanol mixture of 2 mL of 2,2′:6′,2″-terpyridine and an ethanolic solution of chloranilic acid (1 mmol·L^{-1}) was poured into the glass tube without mixing the solutions. Purple crystals began to form at ambient temperature in 2 weeks. One of these crystals was used for X-ray crystallography. Physical measurements were conducted on a polycrystalline powder that was synthesized as follows: An aqueous solution (50 mL) of copper(II) sulfate pentahydrate (0.075 g; 0.3 mmol) was added to an ethanolic solution (50 mL) of 2,2′:6′,2″-terpyridine (0.047 g; 0.2 mmol). The solution was stirred a few minutes, and an ethanolic solution (50 mL) of chloranilic acid (0.062 g; 0.3 mmol) was added. Upon stirring of the mixture, purple powders appeared in 24 h. Yield: 78%. Anal. Calcd for $C_{48}Cl_6Cu_3H_{22}N_6O_{12}$: C, 45.11; H, 1.73; N, 6.58. Found: C, 44.96; H, 1.73; N, 6.39. The homogeneity of the powder sample was confirmed by comparison of the observed and calculated powder diffraction patterns obtained from single-crystal data.

$\{[Cu_2(CA)(terpy)_2(dmso)_2][Cu(CA)_2(dmso)_2](EtOH)\}_n$ **(2).** Compound **1** (0.235 g) was dissolved in 250 mL of dmso. The solution became red purple. To this solution was added 250 mL of ethanol. The mixture was stirred for a few hours and kept at the room temperature. Purple powders appeared in 1 week. Yield: 68%. Anal. Calcd for $C_{58}Cl_6Cu_3H_{52}N_6O_{17}S_4$: C, 42.56; H, 3.20; N, 5.14. Found: C, 41.96; H, 3.00; N, 5.18. Physical measurements were conducted on this polycrystalline powder. For single crystals, 0.100 g of compound **1** was dissolved in dmso (100 mL). This solution (3 mL) was transferred to a glass tube, and then 3 mL of ethanol was poured into the tube without mixing the two solutions. Purple crystals began to form at ambient temperature in 1 month. The homogeneity of the powder sample was confirmed by comparison of the observed and calculated powder diffraction patterns obtained from single-crystal data.

Physical Measurements. Magnetic susceptibility data were recorded over the temperature range from 2 to 300 K in the presence of a magnetic field between 50 and 5000 G with a SQUID susceptometer (Quantum Design, San Diego, CA). All data were corrected for diamagnetism, which was calculated from Pascal's tables. The TIP was assumed to be 60×10^{-6} cm^3 mol^{-1}. Least-squares fitting of the magnetic susceptibility to appropriate equations with Heisenberg Hamiltonian ($H = -J\mathbf{S}_i \cdot \mathbf{S}_i$) were performed. X-ray powder diffraction data were collected on a Rigaku RINT 2000 diffractometer by using Cu Kα radiation.

Crystallographic Data Collection and Refinement of the Structure. Data collection was carried out by a Rigaku AFC7R diffractometer with graphite-monochromated Mo Kα radiation for **1**. For **2**, all measurements were made on a Rigaku Mercury charge-coupled device (CCD) system with graphite-monochromated Mo Kα radiation. Crystallographic data are given in Table 1. The structures were solved by standard direct methods (the *CrystalStructure* crystallographic software package of the Molecular Structure Corp. and Rigaku). Full-matrix least-squares refinements (SHELXL-97)[58] were carried out with anisotropic thermal parameters for all non-hydrogen atoms. All the hydrogen atoms were placed in the calculated positions and fixed. Atomic coordinates are given in Table 2.

Table 1. Crystallographic Data for Compounds **1** and **2**

	1	**2**
formula	$Cu_3C_{48}H_{22}Cl_6N_6O_{12}$	$Cu_3C_{58}H_{52}Cl_6N_6O_{17}S_4$
fw	1278.07	1636.69
cryst system	triclinic	triclinic
space group	$P\bar{1}$ (No. 2)	$P\bar{1}$ (No. 2)
a (Å)	9.168(9)	8.418(3)
b (Å)	10.344(10)	13.341(5)
c (Å)	13.087(5)	15.286(5)
α (deg)	91.34(6)	90.802(9)
β (deg)	96.76(6)	99.959(12)
γ (deg)	111.68(6)	96.043(12)
V (Å^3)	1142.2(16)	1680.5(10)
Z	1	1
ρ(calcd) (g/cm^3)	1.858	1.617
diffractometer	Rigaku AFC7R	Rigaku Mercury CCD
temp (K)	298	200
R_1	0.0628	0.0639
wR_2	0.1878	0.1831
GOF	1.01	1.02

Results and Discussion

Crystal Structures. $\{[Cu_2(CA)(terpy)_2][Cu(CA)_2]\}_n$ **(1).** Crystal structure of **1** is made up of mono- and dinuclear copper(II) units of the formulas $[Cu(CA)_2]^{2-}$ and $[Cu_2(CA)(terpy)_2]^{2+}$, respectively, which are linked by semicoordination of the coordinated oxygen atoms on the CA^{2-} of the monomer to the Cu(II) ion on the dimer unit leading to a one-dimensional chain structure. An ORTEP drawing of the two units in **1** is shown in Figure 1a, and the selected bond distances and angles of the compound are given in Table 2. In the monomer unit, four oxygen atoms from the two CA^{2-} make a square planar environment and the copper atom sits on the inversion center. The oxygen atoms coordinate asymmetrically (1.914(5) Å (Cu(1)−O(1) and Cu(1)−O(1′)), 1.963(5) Å (Cu(1)−O(2), Cu(1)−O(2′)) while the CA dianions have a symmetrical structure which is recognized from the similar C−O distances, 1.276(8) Å (C(1)−O(1)) and 1.282(9) Å (C(2)−O(2)) for coordinated and 1.214(9) Å (C(4)−O(4)) and 1.218(9) Å (C(5)−O(3)) for uncoordinated oxygen atoms. The difference in the Cu−O bond lengths may be due to the weak coordination of O(2) to Cu(2) (vide infra).

On the other hand, each copper(II) ion is coordinated to three nitrogen atoms of one terpy and two oxygen atoms of one CA^{2-} that acts in a bridging bis-bidentate fashion in the dimer unit. The CA^{2-} is situated in a plane nearly orthogonal to that of terpy (84°). Further, the oxygen atom on the CA^{2-} in the monomer unit weakly coordinates to the copper(II) ion.[54,59] Therefore, the geometry around the copper ion may be viewed as elongated octahedral. When the longer Cu−O

(58) Sheldrick, G. M. *SHELEX-97, Program for X-ray Crystal Structure Refinement*; University of Göttingen: Göttingen, Germany, 1997.
(59) Kitagawa, S.; Okubo, T.; Kawata, S.; Kondo, M.; Katada, M.; Kobayashi, H. *Inorg. Chem.* **1995**, *34*, 4790.

Table 2. Selected Bond Distances (Å) and Angles (deg)

Compound **1**			
Cu(1)−O(1)	1.914(5)	Cu(1)−O(2)	1.963(5)
Cu(2)−O(2)	2.707(6)	Cu(2)−O(5)	1.936(5)
Cu(2)−O(6)	2.245(6)	Cu(2)−N(1)	2.049(7)
Cu(2)−N(2)	1.914(6)	Cu(2)−N(3)	2.031(6)
Cl(1)−C(6)	1.734(8)	Cl(2)−C(3)	1.734(8)
Cl(3)−C(9)	1.711(7)	O(1)−C(1)	1.276(8)
O(2)−C(2)	1.282(9)	O(3)−C(5)	1.218(9)
O(4)−C(4)	1.214(9)	O(5)−C(8)	1.273(9)
O(6)−C(7)	1.216(8)	C(1)−C(2)	1.517(10)
C(1)−C(6)	1.371(11)	C(2)−C(3)	1.361(10)
C(3)−C(4)	1.430(11)	C(4)−C(5)	1.563(11)
C(5)−C(6)	1.420(11)	C(7)−C(8)	1.550(10)
C(7)−C(9′)	1.417(10)	C(8)−C(9)	1.390(10)
O(1)−Cu(1)−O(2)	84.1(2)	O(1)−Cu(1)−O(2′)	95.9(2)
O(2)−Cu(2)−O(5)	82.3(2)	O(2)−Cu(2)−O(6)	161.89(17)
O(2)−Cu(2)−N(1)	94.1(2)	O(2)−Cu(2)−N(2)	102.6(2)
O(2)−Cu(2)−N(3)	84.2(2)	O(5)−Cu(2)−O(6)	79.6(2)
O(5)−Cu(2)−N(1)	98.4(2)	O(5)−Cu(2)−N(2)	174.7(3)
O(5)−Cu(2)−N(3)	100.7(2)	O(6)−Cu(2)−N(1)	87.4(2)
O(6)−Cu(2)−N(2)	95.4(2)	O(6)−Cu(2)−N(3)	100.2(2)
N(1)−Cu(2)−N(2)	79.6(3)	N(1)−Cu(2)−N(3)	160.4(3)
N(2)−Cu(2)−N(3)	81.7(3)		
Compound **2**			
Cu(1)−O(1)	1.968(3)	Cu(1)−O(2)	1.949(3)
Cu(1)−O(7)	2.411(5)	Cu(2)−O(5)	1.946(3)
Cu(2)−O(6)	2.355(3)	Cu(2)−O(8)	2.347(3)
Cu(2)−N(1)	2.038(3)	Cu(2)−N(2)	1.931(3)
Cu(2)−N(3)	2.032(3)	Cl(1)−C(3)	1.729(4)
Cl(2)−C(6)	1.737(5)	Cl(3)−C(9)	1.725(3)
Cl(3)−C(9)	1.725(3)	O(1)−C(1)	1.276(5)
O(2)−C(2)	1.280(4)	O(3)−C(4)	1.227(5)
O(4)−C(5)	1.228(5)	O(5)−C(7)	1.276(4)
O(6)−C(8)	1.236(4)	C(1)−C(2)	1.510(5)
C(1)−C(6)	1.377(6)	C(2)−C(3)	1.372(5)
C(3)−C(4)	1.416(5)	C(4)−C(5)	1.532(6)
C(5)−C(6)	1.411(6)	C(7)−C(8)	1.530(5)
C(7)−C(9′)	1.370(4)	C(8)−C(9)	1.421(5)
O(1)−Cu(1)−O(2)	83.38(12)	O(1)−Cu(1)−O(2′)	96.62(12)
O(1)−Cu(1)−O(7)	87.4(2)	O(1)−Cu(1)−O(7′)	92.6(2)
O(2)−Cu(1)−O(7)	87.64(19)	O(2)−Cu(1)−O(7′)	92.36(19)
O(5)−Cu(2)−O(6)	75.81(10)	O(5)−Cu(2)−O(8)	91.60(11)
O(5)−Cu(2)−N(1)	99.51(13)	O(5)−Cu(2)−N(2)	178.68(12)
O(5)−Cu(2)−N(3)	100.06(13)	O(6)−Cu(2)−O(8)	166.92(10)
O(6)−Cu(2)−N(1)	86.73(12)	O(6)−Cu(2)−N(2)	102.95(11)
O(6)−Cu(2)−N(3)	96.42(12)	O(8)−Cu(2)−N(1)	91.98(14)
O(8)−Cu(2)−N(2)	89.61(12)	O(8)−Cu(2)−N(3)	89.17(14)
N(1)−Cu(2)−N(2)	79.94(13)	N(1)−Cu(2)−N(3)	160.36(13)
N(2)−Cu(2)−N(3)	80.46(14)		

distance is viewed as the apical direction of an elongated octahedron, one of the oxygen atom on the bridging CA^{2-} and the three nitrogen atoms define the basal plane. The Cu−O distance on the plane (Cu(2)−O(5), 1.936(5) Å) is shorter than that of the apical one (Cu(2)−O(6), 2.245(6) Å) indicating the asymmetric coordination mode of the CA^{2-} dianion. Such asymmetrical coordination of the CA^{2-} dianion is also reflected in the distances of the C−O bonds. This feature is similar to that of $[Cu_2(terpy)(CA)](PF_6)_2$, which has a discrete dimeric structure, and the C−O bonds of equal length are located in ortho positions.[45] The N−Cu−N angles are close (∼80°) and rigidly imposed by the terpy ligand.

The assembled structure of **1** is shown in Figure 1b. The zigzag chain exhibits regular alternation of the monomer and the dimer units. Therefore, two kinds of modules are connected alternatively to form the chain motif in **1** by a semicoordination-bonding interaction (Cu(2)−O(2), 2.707(6) Å). The intradimer Cu−Cu separation is 7.888(6) Å, while the monomer−dimer Cu−Cu distance is 3.741(4) Å. Additionally, the chain structure is supported by several secondary bonding interactions: $\pi-\pi$ stacking interactions (C(1)−C(10), 3.312(12) Å; C(2)−N(1), 3.220(10) Å); Cu−O interactions (Cu(1)−O(5), 2.969(6) Å); Cl−C contacts (Cl(3)−C(2′), 3.051(8); Cl(2)−C(19), 3.380(9) Å); CH−Cl hydrogen-bonding interaction (C(23)−Cl(1′), 3.567(11) Å). The contact of 3.05 Å between the Cl atom on the monomer unit and the C atom of the terpy ligand on the dimer unit is particularly close, significantly less than the sum of the van der Waals radii; indeed this contact would be short even for a carbon−carbon contact.[18,47,52,60−63]

Moreover, the chains are assembled to a three-dimensional structure by $\pi-\pi$ stacking interactions, Cl−C contacts (Cl(1)−C(7′), 3.364(8) Å) and CH−Cl hydrogen-bonding interactions (Cl(2)−C(12′), 3.700(10) Å) (Figure 1d), CH−O hydrogen-bonding interactions (O(1)−C(11′), 3.595(11) Å), and Cl−Cl contact (Cl(2)−Cl(2′), 3.314(4) Å) shown in Figure 1c,d.[64−66]

$\{[Cu_2(CA)(terpy)_2(dmso)_2][Cu(CA)_2(dmso)_2](EtOH)\}_n$ (2). The crystal structure of the compound **2** is made up of mono- and dimeric units of the formula $\{[Cu(CA)_2(dmso)_2]^{2-}$ and $[Cu_2(CA)(terpy)_2(dmso)_2]^{2+}$, respectively. An ORTEP drawing of the compound **2** is shown in Figure 2a, and the selected bond distances and angles are given in Table 2. The geometry around the copper ion of the monomer anion is a distorted octahedron involving the four oxygen atoms of two CA^{2-} anions and the two oxygen atoms from dmso molecules which are trans to each other. The dmso molecules disorder in two positions. The environment of the copper atom consists of the four short in-plane bonds and the two long axial bonds, giving rise to a "4 + 2" type of configuration. The oxygen atoms on the CA^{2-} dianions coordinate symmetrically (1.968(3) Å (Cu(1)−O(1) and Cu(1)−O(1′)); 1.949(3) Å (Cu(1)−O(2), Cu(2)−O(2′)) reflecting that the CA dianions have a symmetrical structure which is recognized from the C−C and C−O distances, 1.276(5) Å (C(1)−O(1)) and 1.280(4) Å (C(2)−O(2)). These features are different from those of the monomer unit on **1**, and the differences are attributed to the semicoordination bonding interactions between the monomer and the dimer in **1** described above. Moreover, the in-plane Cu−O distances of **2** are longer than those of **1** due to the apical coordination of the dmso molecules, and thus, the apical coordination of the dmso molecule forces the ligand field strength of the basal plane to weaken.

On the other hand, each copper(II) ion in the dimer is coordinated to an oxygen atom of dmso, three nitrogen atoms of one terpy, and two oxygen atoms of one CA^{2-} that acts in a bridging bis-bidentate fashion. The CA^{2-} dianion is situated in a plane nearly orthogonal to that of terpy (85°).

(60) Andersen, E. K. *Acta Crystallogr.* **1967**, *22*, 191.
(61) Price, S. L.; Stone, A. J.; Lucas, J.; Rowland, R. S.; Thornley, A. E. *J. Am. Chem. Soc.* **1994**, *116*, 4910.
(62) Gray, L.; Jones, P. G. *Z. Naturforsch.* **2002**, *57b*, 61.
(63) Gray, L.; Jones, P. G. *Z. Naturforsch.* **2002**, *57b*, 73.
(64) Desiraju, G. R.; Steiner, T. R. *The Weak Hydrogen Bond in Structural Chemistry and Biology*; Oxford University Press: Oxford, U.K., 1999.
(65) Steiner, T. *Angew. Chem., Int. Ed.* **2002**, *41*, 48.
(66) Meyer, E. A.; Castellano, R. K.; Diederich, F. *Angew. Chem., Int. Ed.* **2003**, *42*, 1210.

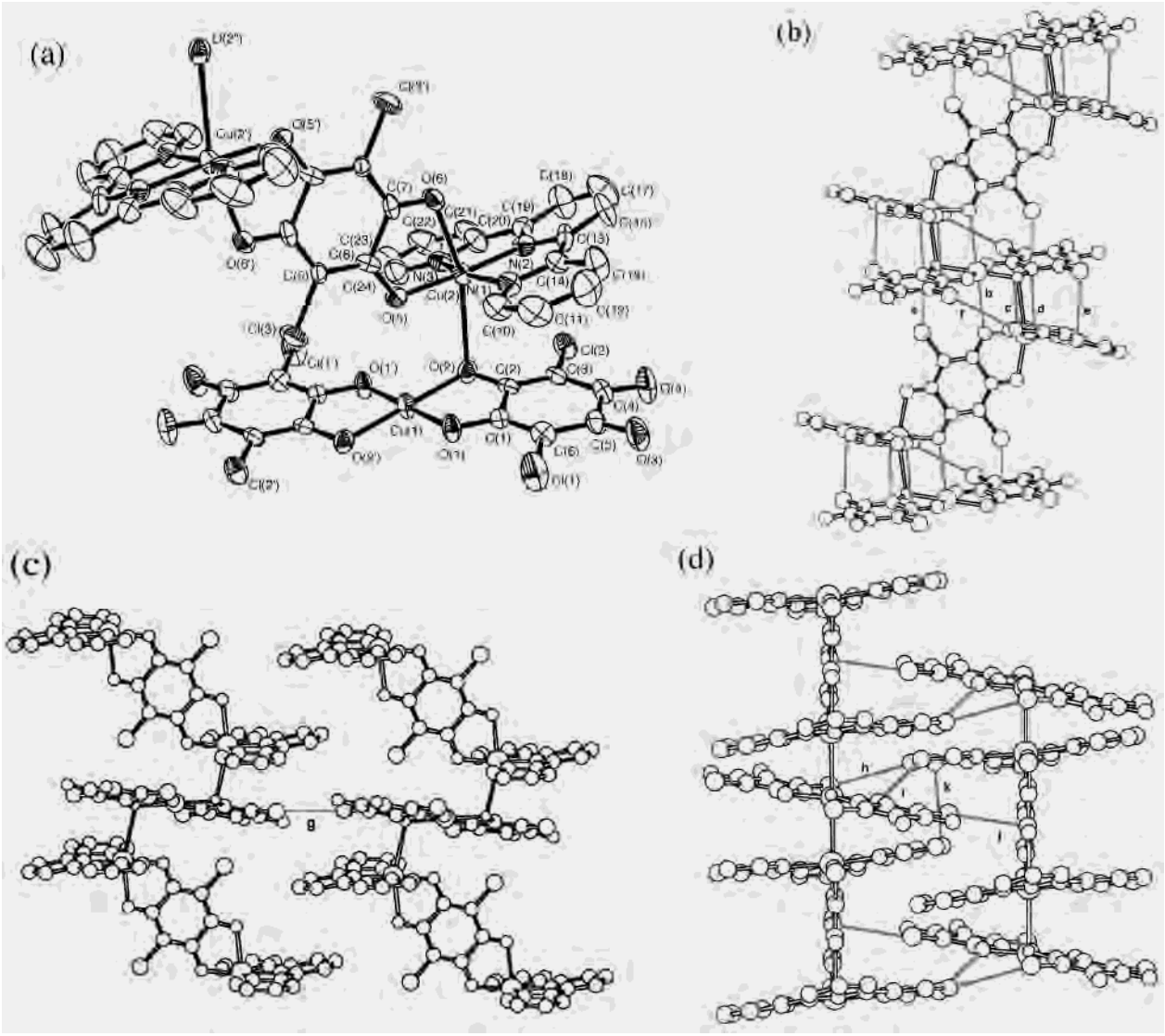

Figure 1. Crystal structure of **1**. (a) ORTEP view of the molecular fragment of the structure showing the immediate environments of the copper atoms together with the atom-labeling scheme. (b) Perspective view of the structure showing the formation of the polymeric chain propagated along the crystallographic *c*-axis. Gray lines denote weak bonding interactions in the chain: $a = 3.05$, $b = 2.97$, $c = 3.31$, $d = 3.22$, and $e = 3.38$ Å; CH−Cl hydrogen bond (the numerical value is a D···A distance), $f = 3.57$ Å. (c) Cl−Cl contact between the chains in **1** ($g = 3.31$ Å). (d) Hydrogen-bonding network: $h = 3.70$, $i = 3.60$ Å (the numerical values are D···A distances); Cl−C contact between the chains, $j = 3.36$ Å; $\pi-\pi$ stacking interaction between the chains, $k = 3.56$ Å.

The geometry around the copper ion may be viewed as distorted octahedral. When the longer Cu−O distance is viewed as the apical direction of a distorted octahedron, one of the oxygen atoms (O(5)) on the bridging CA^{2-} and the three nitrogen atoms define the basal plane. The Cu−O distance on the plane (Cu(2)−O(5), 1.946(3) Å) is shorter than that of the apical one (Cu(2)−O(6), 2.355(3) Å) indicating the asymmetric coordination mode of the bridging CA^{2-} dianion. The N−Cu−N angles are similar to those of **1** and close (∼80°) and rigidly imposed by the terpy ligand. The intradimer Cu−Cu distance is 8.057(2) Å, the value of which is longer than that of the dimer in **1** due to the longer Cu−O distances. Each dmso molecule coordinates to the sixth position of the octahedron, while the one of the oxygen atom of the CA dianion in the monomer coordinates to this position for **1**. Therefore, the apical coordination also weakens the ligand field strength of the basal plane. Furthermore, the solvent molecules prevent the coordination of the different modules to attach together to form the extended network.

While the intramolecular distances do not provide any surprises, the intermolecular contacts in this structure mediates the formation of a motif whose nature and symmetry are far removed from the shapes of the modules. Interestingly, the dimers form a layer extended to the *xy* plane (Figure 2b). The layers are supported by secondary but efficient three kinds of interactions: (1) The adjacent dimers are stacked on each other with coordinated terpy, the distances of the neighbor C(17)−C(19′), C(17)−C(23′), and C(19)−C(21′) being 3.532(6), 3.604(7), and 3.506(6) Å, respectively, to support the layer. (2) The hydrogen bonds (C(17)−O(6′), 3.155(5) Å; C(21)−O(8′), 3.227(6) Å) occur between the carbon atom on the terpy and the coordinated oxygen atom of CA^{2-} on the nearest neighbor dimer and between the carbon atom on the terpy and the coordinated oxygen atom of dmso on the nearest neighbor dimer,

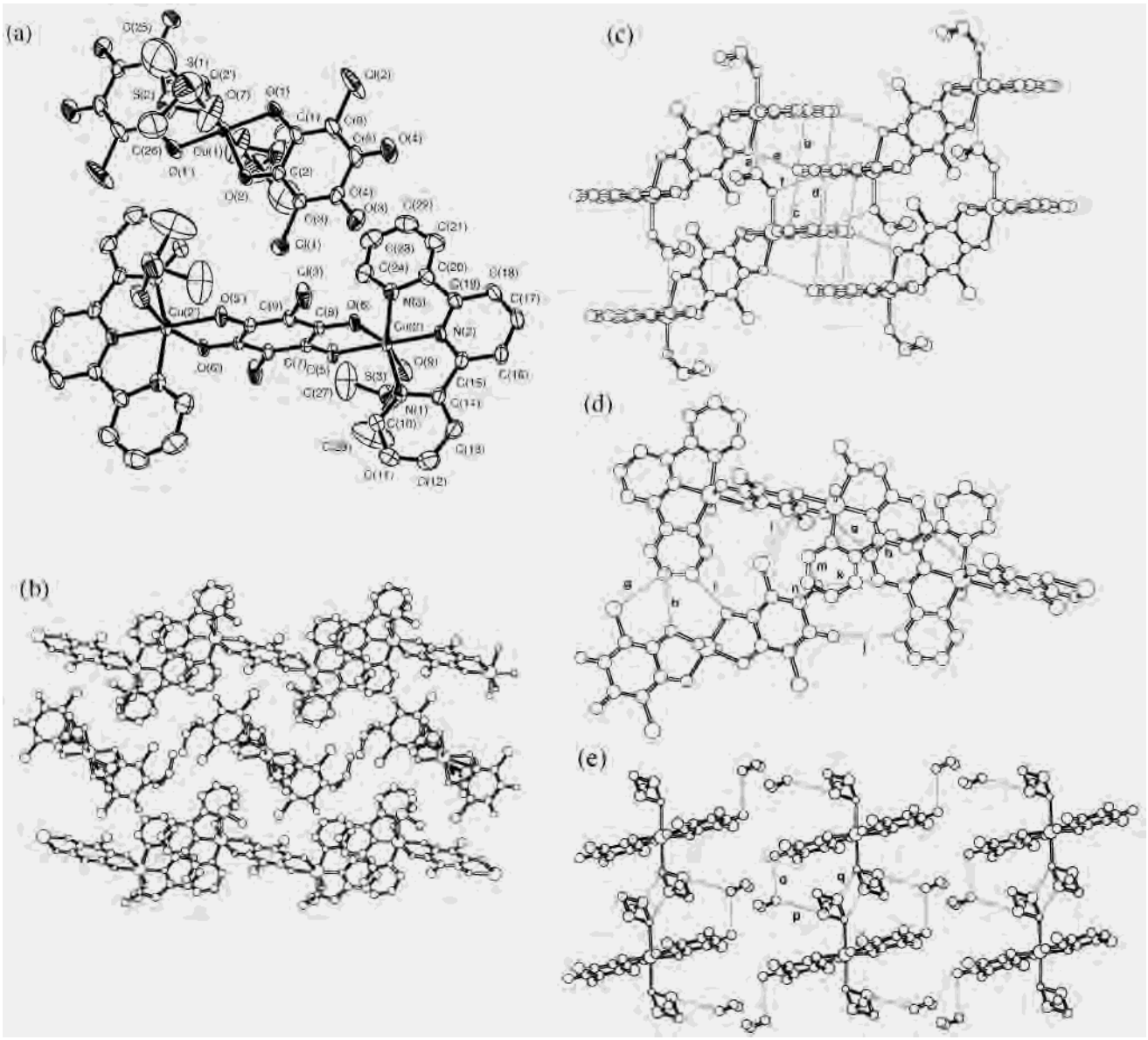

Figure 2. Crystal structure of **2**. (a) ORTEP view of the molecular fragment of the structure **2** showing the immediate environments of the copper atoms together with the atom-labeling scheme. (b) Assembled structure. (c) Layer structure of $[Cu_2(CA)(terpy)_2(dmso)_2]^{2+}$ module. Gray lines denote weak bonding interactions in the layer: $a = 3.52$, $b = 3.53$, $c = 3.60$, $d = 3.51$, $e = 3.16$, and $f = 3.23$ Å (the numerical values of e and f are D···A distances). (d) Weak bonding interaction between the modules. Hydrogen bonds: $g = 3.59$, $h = 3.41$, $i = 3.36$, $j = 3.36$, and $k = 3.05$ Å (the numerical values are D···A distances); Cl−C or $\pi-\pi$ stacking interactions, $l = 3.46$, $m = 3.35$, and $n = 3.39$ Å. (e) Hydrogen-bonding network in the $[Cu(CA)_2(dmso)_2]^{2-}$ module: $o = 3.11$, $p = 3.54$, and $q = 3.36$ Å.

respectively. (3) The contact of 3.516(6) Å between S(3) atom on dmso and C(12) of the terpy ligand on the adjacent unit is found. Moreover, the monomer anion and ethanol molecules are introduced in the layer (Figure 2c). The introduced monomer is supported by four kinds of secondary bonding interactions to the dimers shown in Figure 2d: stacking interactions (C(4)−C(23), 3.385(7) Å; O(3)−C(24), 3.346(6) Å); Cl−C contact (Cl(1)−C(8), 3.461(4) Å); CH−Cl hydrogen-bonding interaction (C(12)−Cl(2′), 3.588(6) Å); CH−O hydrogen-bonding interactions (O(1)−C(12′), 3.413(6) Å; O(2)−C(11′), 3.358(6) Å; O(3)−C(16′), 3.048(5) Å; O(4)−C(13′), 3.361(6) Å). The interstitial ethanol molecules disorder in two positions and are hydrogen bonded to the oxygen atom of the coordinated dmso or the oxygen atoms on the CA^{2-} dianion (O(9)−O(4), 3.113(12) Å; O(9)−S(2′), 3.542(15) Å) (Figure 2e). The sulfur atom on the coordinated dmso contacts the nearest neighbor oxygen atom on the adjacent dmso molecule to form a one-dimensional structure between the layer (S(1)−O(7′), 3.357-(7) Å).

Solvent Control in the Assembled Structures. As concluded from the structural analysis, significant differences between complexes **1** and **2** related to the use of different solvent systems are found while there are two kinds of modules, monomer and dimer units, which are built from the common synthon, Cu−CA, in both of the compounds **1** and **2** (Scheme 2).

1 exhibits a one-dimensional structure which leads to regular alternation of the monomer and the dimer units: two kinds of modules connect to each other by semicoordinating

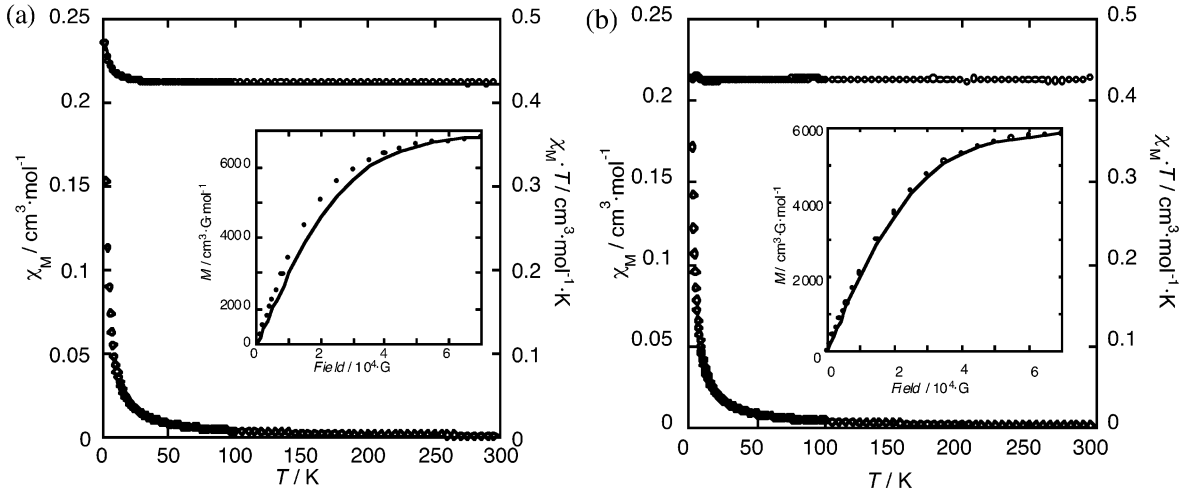

Figure 3. Plots of χT and $1/\chi$ vs T for (a) **1** (a) and (b) **2**. Solid lines: theoretical fits of the data with the parameters listed in the text. Insets: Field dependence of the magnetizations at 2.0 K. Solid lines denote Brillouin function for a spin doublet.

Scheme 2

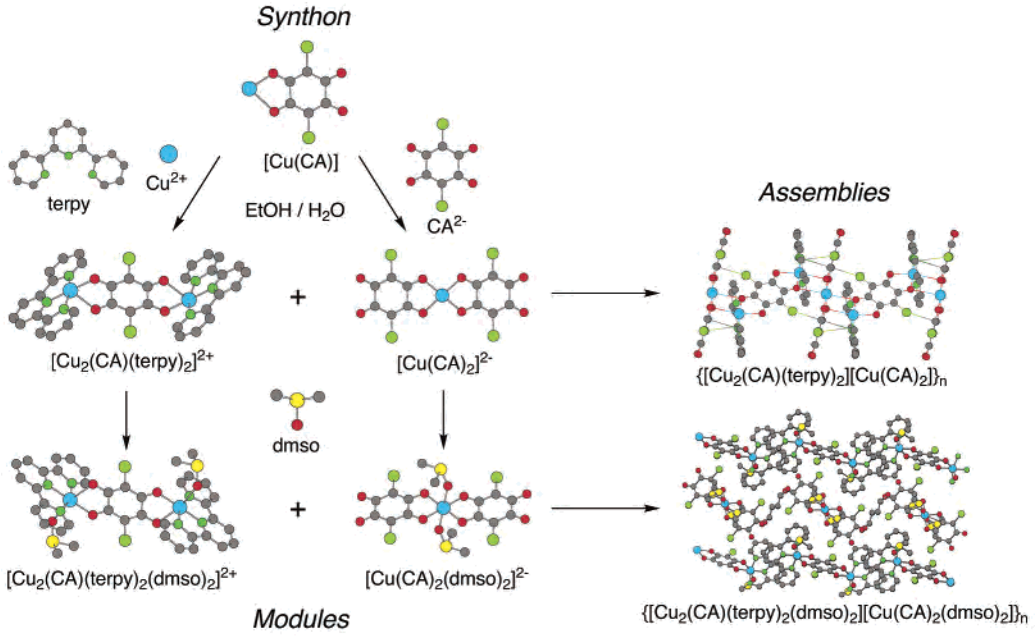

interaction and additional but efficient secondary bonding interactions. Compound **2** contains discrete dimer and monomer units in which dmso molecules coordinate to both of the copper(II) ions. The solvent molecules prevent the coordination of the different modules to form the extended network but allow the aggregation by the secondary bonding interactions between the modules, giving rise to a 3D network. Therefore, the solvent molecules coordinated in the modules clearly control the mode of assembly in the solid.

Magnetic Properties. The magnetic properties of **1** under the form of the $\chi_M T$ product versus T (χ_M being the magnetic susceptibility/one copper(II) ions) is shown in Figure 3a. $\chi_M T$ at 300 K is equal to 0.42 cm^3·mol^{-1}·K, a value of which is as expected for one magnetically isolated spin doublet. This value remains practically constant through cooling from 300 to 30 K, and it increases gradually at lower temperatures to attain a value of 0.46 cm^3·mol^{-1}·K at 2.0 K. This curve reveals the ferromagnetic coupling in **1**. As the structure of **1** consists of the monomer unit and the dimer unit, the magnetic interactions in the chain is denoted J_a and J_b shown in Scheme 3.

The magnetic interaction in a similar dimeric module of Cu−CA−Cu in which the magnetic orbitals, of $d_{x^2-y^2}$ type, are essentially localized in the basal planes and lie perpendicular to the chloranilate plane is relatively small ($|J| < 0.5$ cm^{-1}),[35,38,42−45,48] and it is easy to conclude that the magnetic interaction mainly occurs between the Cu ions on the dimer and the monomer moieties; that is, $|J_a| > |J_b|$. From this point of view, the compound looks like an assembly of trimers with relatively larger magnetic interaction (J_a) connected through weak interaction (J_b). The attempt to model the magnetic susceptibility is done with a simple ABA

Scheme 3

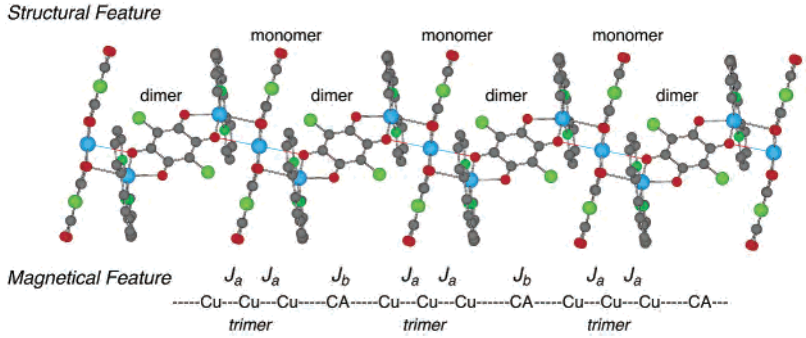

Scheme 4

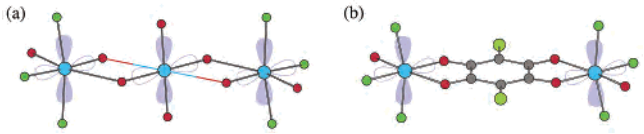

linear trinuclear model with mean-field approximation based on the following equations:[21,67]

$$\chi_{\text{trimer}} = \frac{N\mu_B^2}{kT}\frac{g_{1/2,1}^2 + g_{1/2,0}^2 \exp[J_a/kT] + 10g_{3/2,1}^2 \exp[3J_a/2kT]}{1 + \exp[J_a/kT] + 2\exp[3J_a/2kT]} \quad (1)$$

$$\chi = \frac{\chi_{\text{trimer}}}{1 - \frac{2zJ_b}{Ng^2\mu_B^2}\chi_{\text{trimer}}} \quad (2)$$

$$g_{1/2,1} = (4g_{\text{dimer}} - g_{\text{monomer}})/3 \quad (3)$$

$$g_{3/2,1} = (2g_{\text{dimer}} - g_{\text{monomer}})/3 \quad (4)$$

$$g_{1/2,0} = g_{\text{monomer}} \quad (5)$$

$$g^2 = g_{1/2,1}^2 + g_{3/2,1}^2 + g_{1/2,0}^2 \quad (6)$$

In the above equations, g_{dimer} and g_{monomer} are the g-factors of the copper ions on the dimer unit and on the monomer unit, respectively. The best fit parameters are $J_a = 2.36$ cm^{-1}, $zJ_b = -0.68$ cm^{-1}, $g_{\text{dimer}} = 2.11$, and $g_{\text{monomer}} = 2.13$. The intratrimer ferromagnetic coupling observed in **1** is in agreement with the trimeric conformation: bridged oxygen atoms are involved in the exchange pathway. The relative orientation of the metal-centered magnetic orbitals within the chain is depicted in Scheme 4a. The magnetic orbital at each copper atom is defined by the short equatorial bonds. There it can be seen that the out-of-plane exchange pathway is involved in the Cu−O−Cu−O−Cu fragment. Therefore, ferromagnetic couplings would be predicted, as observed, and zJ_b can be attributed to the dominant intertrimer interaction. As each trimer is surrounded by two trimers within a chain, $z = 2$ and $J_b = -0.34$ cm^{-1}. The intertrimer antiferromagnetic interaction is weaker than the exchange interaction for $[Cu(CA)]_n$, which has a planar ribbon structure (-12.3 cm^{-1}), and comparable to that for β-$\{[Cu(CA)(H_2O)_2]$-$(dmpyz)\}_n$,[48] in which the magnetic orbital lies perpendicular to the chloranilate plane, suggesting that the magnetic orbital $d_{x^2-y^2}$ is parallel to the plane of Cu−terpy, as predicted from the structure.[35,38,48] This is also made clear in the comparison with $[Cu_2(terpy)_2(CA)]^{2+}$, $[Cu_2(Me_2dien)_2(CA)]^{2+}$, and $[Cu_2(Me_2dien)_2(dhbq)]^{2+}$, in which the copper(II) ion has a five-coordinated geometry with a tridentate end-cap ligand, and compound **2** (vide infra).[42−45]

The variation of $\chi_M T$ versus T for **2** is shown in Figure 3b. $\chi_M T$ at 300 K is equal to 0.425 cm^3·mol^{-1}·K, a value of which is as expected for one magnetically isolated spin doublet. This value remains practically constant through cooling from 300 K up to 2 K, which reveals the paramagnetic state of **2**. As the structure of **2** consists of the monomer and the dimer, which are linked only by electrostatic forces, van der Waals interactions, and an extensive network of hydrogen bonds, the magnetic interactions between the components in **2** are smaller than that of the chain in **1**; thus, the magnetic interaction mainly operates in the dimer unit. However, no intradimer coupling was observed in **2**, which is in agreement with the dimeric conformation shown in Scheme 4b: the magnetic orbital also lies perpendicular to the chloranilate plane, suggesting that the magnetic orbital $d_{x^2-y^2}$ is parallel to the plane of Cu−terpy. The above magnetic behavior of **2** is slightly different from that in **1**, which may be due to the longer Cu−Cu distance (**1**, 7.89 Å; **2**, 8.06 Å) and the planarity of the basal planes. Owing to the higher planarity of the basal plane of the dimer in **2**, the mixing of the d_{z^2} orbital, which directs to the oxygen atom of the CA^{2-} ion, with the magnetic orbital $d_{x^2-y^2}$ orbital is smaller than that in **1**. These features account for residual coupling in **1**.[35,38] The mixing of the magnetic orbital on the copper ion modifies the residual spin densities on the coordinated oxygen atoms of CA^{2-} and hence the magnitude of the intraligand exchange coupling.

Conclusion

In this study, it is shown how the common synthon based on copper chloranilate can be used for the construction of new types of metal-assembled complexes, which consist of different modules. There is a structural diversity among the copper chloranilate complexes. The assembled structures are easily controlled by the selection of the solvent. The above

(67) Kahn, O. *Molecular Magnetism*; VCH: New York, 1993.

results show that the present approach is a successful procedure to prepare new types of metal-assembled complexes and the advances in the design of them will depend on the crystal engineering that involves the development of convenient synthetic strategies leading to a better control of the supramolecular structure of the materials.

Acknowledgment. This research was supported by a Grant-in-Aid for Scientific Research (No. 15550050) and by Grant-in-Aids for Scientific Research on Priority Areas (Nos. 413 and 417) from the Ministry of Education, Culture, Sports, Science, and Technology of Japan.

Supporting Information Available: Figures S1 and S2, representing powder XRD diagrams of **1** and **2**, and X-ray crystallographic files in CIF format. This material is available free of charge via the Internet at http://pubs.acs.org.

IC035044Y